

BIASMIX-FINANCE: POST-GENERATION KYC GUARDRAILS FOR LLM PORTFOLIO ADVICE

000
001
002
003
004
005 **Anonymous authors**
006 Paper under double-blind review
007
008
009
010

ABSTRACT

011 Large language models (LLMs) can generate plausible-sounding ETF portfolios
012 while silently violating basic KYC-style constraints on risk, fees, and diversification.
013 We study a model-agnostic, asset-agnostic *post-generation guardrail*
014 pipeline: (i) enforce a strict JSON allocation schema, (ii) validate allocations
015 against numeric caps, and (iii) when violations occur, *deterministically* project the
016 output to the nearest feasible portfolio via a convex quadratic program (QCQP).
017 We introduce **BiasMix-Finance (Mini)**, a compact stress-test benchmark for *con-*
018 *strained decision-making under biased LLM generations*, with a 16-ETF universe,
019 three investor profiles, and eight bias prompts. Across three models and three in-
020 ference modes (direct, critique, self-consistency), first-pass generations violate at
021 least one cap in **47.6–85.7%** of test cases (**67.2%** pooled), but the convex projec-
022 tion layer reduces *final feasibility violations to 0%* while requiring only a *small*
023 *correction distance* (test pooled median $D = \|w^* - w_0\|_2 = 0.066$), indicating
024 that the guardrail typically preserves the intent of the original allocation. We re-
025 port violation rates and correction distances with confidence intervals, and paired
026 model comparisons with multiple-testing correction. To support reproducibility,
027 we will release the dataset, prompts, caps, and code in an anonymous repository
028 (URL withheld for double-blind review).

1 INTRODUCTION

029
030 Large language models (LLMs) are increasingly used to generate financial summaries, recom-
031 mendations, and portfolio allocations (Wu et al., 2023; Yang et al., 2023). However, in regulated domains
032 the output must satisfy *hard* suitability and diversification constraints (e.g., concentration limits, fee
033 ceilings, and risk caps) that resemble KYC/suitability guardrails (Jagannathan & Ma, 2003; Boyd
034 & Vandenberghe, 2004). Prompting and reasoning-mode variations (e.g., critique, self-consistency)
035 are inherently probabilistic and cannot guarantee constraint satisfaction on every run (Wei et al.,
036 2022; Wang et al., 2022; Yao et al., 2023). This motivates **post-generation enforcement**: we treat
037 the LLM output as a draft allocation and apply deterministic verification and repair to ensure com-
038 pliance (Rao et al., 2023; Meta, 2023; Ribeiro et al., 2020; Dror et al., 2018). Crucially, our goal is
039 *not* to solve a classical portfolio-optimization problem (e.g., maximizing risk-adjusted return under
040 constraints) (Markowitz, 1952; Black & Litterman, 1992; Goldfarb & Iyengar, 2003). Instead, we
041 study an *auditing and repair* problem: how to reliably detect and minimally correct *irrational or*
042 *constraint-violating* allocations produced by an LLM, while preserving the model’s intended alloca-
043 tion structure as much as possible (Ribeiro et al., 2020; Bender et al., 2021; Raji et al., 2020). More
044 broadly, this setting instantiates a common *alignment and robustness* problem: an LLM produces
045 a plausible *decision* artifact, but correctness depends on satisfying external constraints that must be
046 verified by deterministic checks (Ouyang et al., 2022; Bai et al., 2022). Because these constraints
047 are externally specified and mechanically checkable, the task is a natural testbed for *post-hoc veri-*
048 *fication and repair* pipelines that are model-agnostic and transferable to other constrained decision-
049 making domains (e.g., resource allocation, scheduling, or policy compliance). We study a controlled
050 portfolio-allocation setting: given an ETF universe and a scenario describing (i) a risk profile with
051 caps and (ii) a bias-inducing context (e.g., “small-cap hype”), the LLM emits portfolio weights
052 under a strict JSON schema. A key challenge is that biased or preference-shaping contexts can
053 systematically push generations toward concentrated, high-volatility, or otherwise non-compliant
allocations. To evaluate guardrails under these realistic failure modes, we adopt a **bias-induction**

methodology: we programmatically generate scenarios that combine standardized risk profiles with bias “recipes” (e.g., anchoring on a sector, FOMO tilts, inertia, fee neglect), producing a stress-test suite for constraint-violating drafts. We then measure constraint violations *before* repair and the magnitude of correction required *after* repair. Our goal is to quantify how much prompt reasoning modes reduce violations *prior* to enforcement, and how much post-hoc guardrails must change the portfolio to make it compliant. In this sense, we treat BiasMix-Finance (Mini) as a stress-test benchmark for *constrained decision-making under biased generations*, complementing broader evaluation efforts in safe and reliable LLM deployment. To verify that BiasMix prompts elicit the intended behavioral tilts, Appendix Table 6 shows representative first-pass LLM outputs (held-out test) for each bias recipe.

Contributions.

- **Bias-inducing evaluation suite for financial guardrails.** We construct 72 scenario instances (train/dev/test) that combine three risk profiles with eight behavioral “bias recipes” and three random seeds, over a fixed 16-ETF universe. This controlled design isolates how different prompts and models respond to the same constraints and bias contexts, and makes bias induction itself a reproducible evaluation primitive for constrained decision-making under LLM outputs.
- **Post-generation constraint enforcement for LLM portfolio drafts.** We formalize the feasible set induced by volatility, fee, HHI concentration, and max single-asset/sector caps, and compute the nearest feasible portfolio via a constrained quadratic program, solved with standard convex optimization tools (Boyd & Vandenberghe, 2004; Diamond & Boyd, 2016; Stellato et al., 2020).
- **Reproducible statistical evaluation across splits, models, and modes.** We report per-cap violation rates with Wilson 95% confidence intervals (Wilson, 1927), correction-distance and metric-delta confidence intervals via bootstrap (Efron & Tibshirani, 1993), and paired model comparisons on correction distance with Wilcoxon tests plus BH-FDR correction (Wilcoxon, 1945; Benjamini & Hochberg, 1995).

2 PROBLEM SETUP

Universe. Let n denote the number of ETFs in the universe (here $n = 16$) and let $w \in \mathbb{R}^n$ denote portfolio weights.

Scenario. Each scenario provides (i) a risk profile with caps and (ii) a bias context string intended to nudge the model toward potentially non-compliant allocations. Caps include an annualized volatility ceiling σ_{cap} , a weighted-average expense ratio ceiling f_{cap} , a concentration ceiling h_{cap} based on the Herfindahl–Hirschman Index (HHI) (Herfindahl, 1950; Hirschman, 1964), and max single-asset and max single-sector weight caps. Such constraints are standard in constrained portfolio construction and are commonly studied as practical overlays on mean–variance style allocations (Markowitz, 1952; Jagannathan & Ma, 2003).

Model output. The LLM emits a draft portfolio w_0 (JSON with nonnegative weights that sum to 1). We compute summary metrics: risk $\sigma(w) = \sqrt{w^\top \Sigma w}$ (Markowitz, 1952), fee $\text{WAER}(w) = \sum_i w_i \cdot \text{fee}_i$, and concentration $\text{HHI}(w) = \sum_i w_i^2$.

Feasible set. Let \mathcal{C} be the set of portfolios satisfying all caps. A draft is *violating* if $w_0 \notin \mathcal{C}$.

Post-generation enforcement. When w_0 violates any cap, we compute the nearest feasible portfolio

$$w^* = \arg \min_w \|w - w_0\|_2^2 \quad \text{s.t.} \quad w \in \mathcal{C}, \quad (1)$$

and define the correction distance as $D = \|w^* - w_0\|_2$ (Euclidean/L2 distance). Projection operators are a standard way to enforce feasibility under convex constraints (Boyd & Vandenberghe, 2004; Duchi et al., 2008), and related portfolio work often uses robust or constrained formulations to stabilize allocations under estimation error (Black & Litterman, 1992; Goldfarb & Iyengar, 2003; Ben-Tal et al., 2009).

108 **3 RELATED WORK**

110 **LLMs for finance.** Domain-specific financial LLMs such as BloombergGPT (Wu et al., 2023)
 111 and open, community-driven efforts like FinGPT (Yang et al., 2023) demonstrate strong capability
 112 on financial NLP tasks. Our focus differs: we study *hard constraint compliance* for portfolio-weight
 113 outputs rather than text generation accuracy.
 114

115 **Guardrails, auditing, and post-hoc verification.** Safety and controllability toolkits (e.g., NeMo
 116 Guardrails (Rao et al., 2023)), safety classifiers (e.g., Llama Guard (Meta, 2023)), and instruc-
 117 tion/alignment methods such as RLHF and Constitutional AI (Ouyang et al., 2022; Bai et al., 2022)
 118 primarily aim to filter unsafe content or enforce conversational policies. A complementary line of
 119 work emphasizes *auditing* and *verification* of LLM outputs, especially in high-stakes settings: rather
 120 than trusting a single generation, systems instrument the generation process with structured outputs,
 121 validation checks, and feedback loops (Ribeiro et al., 2020; Dror et al., 2018). Constrained genera-
 122 tion methods provide decoding-time guarantees by enforcing lexical or structural constraints during
 123 generation (Hokamp & Liu, 2017). In contrast to content safety, our setting requires satisfying
 124 quantitative constraints that are naturally expressed as convex restrictions over portfolio weights;
 125 this motivates optimization-based post-processing as an auditable repair layer rather than purely
 126 text-level controls (Boyd & Vandenberghe, 2004).

127 **Structured generation and constrained outputs.** A practical prerequisite for auditing is that
 128 model outputs are machine-checkable. Prior work on structured outputs (e.g., JSON/function-style
 129 interfaces) and constrained generation motivates enforcing schemas so downstream validators can
 130 reliably parse and evaluate outputs. Our pipeline adopts this principle by requiring a strict JSON
 131 schema for allocations, enabling deterministic constraint checking and repair.
 132

133 **Constrained portfolio optimization.** Classical mean–variance optimization (Markowitz, 1952)
 134 and later robust/regularized variants (Jagannathan & Ma, 2003) motivate using covariance structure
 135 and explicit constraints in portfolio construction. Our work uses these tools as a *repair operator*
 136 applied to an LLM draft, aligning with the broader view that LLM outputs may require deterministic
 137 verification in high-stakes domains. Unlike traditional optimization, we do not assume the portfolio
 138 is being constructed from first principles to maximize an objective; instead, we minimize deviation
 139 from the model’s proposal while enforcing KYC-style caps.
 140

141 **Reasoning modes and sampling.** Prompting strategies such as chain-of-thought (Wei et al., 2022)
 142 and self-consistency (Wang et al., 2022) can improve reasoning reliability but remain stochastic. We
 143 therefore treat mode comparisons as empirical outcomes and quantify uncertainty with confidence
 144 intervals and paired tests, and we position deterministic post-generation verification/repair as the
 145 mechanism that guarantees compliance regardless of prompting mode.
 146

147 **4 METHODOLOGY**

148 Figure 1 summarizes the end-to-end BiasMix-Finance pipeline from scenario construction to deter-
 149 ministic feasibility via projection (Boyd & Vandenberghe, 2004; Ribeiro et al., 2020).
 150

151 **4.1 UNIVERSE AND SCENARIOS**

153 We construct a synthetic-but-controlled scenario suite over a fixed ETF universe of $n =$
 154 16 liquid funds: SPY, VEA, VWO, VGT, XLE, XLF, XLV, XLY, XLP, XLI, XLRE,
 155 IWM, AGG, LQD, IEF, GLD. Each scenario specifies an *as-of* date (we use 2025-09-30),
 156 a risk profile (Conservative/Moderate/Aggressive), and a *BiasMix* recipe that nudges the model to-
 157 toward a known behavioral bias (e.g., “anchor tech”, “FOMO energy”, “small-cap hype”). Recipes
 158 are expressed as short natural-language preferences (not hard constraints) so that first-pass outputs
 159 can be either feasible or infeasible. This design parallels behavioral stress testing in NLP evalua-
 160 tion: the goal is to systematically elicit failure modes under controlled perturbations (Ribeiro et al.,
 161 2020). We generate 72 scenarios across 3 profiles and 8 bias recipes, with *three* random seeds per
 (profile, recipe) cell; split sizes are train/dev/test = 36/15/21, balanced across the three risk profiles

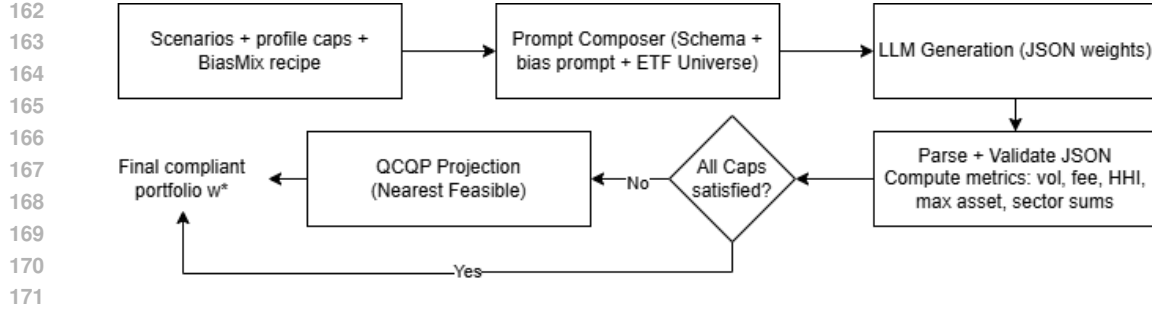


Figure 1: **End-to-end pipeline.** BiasMix scenario + bias recipe are composed into a structured prompt. The LLM generates draft weights (JSON). We validate JSON and compute portfolio metrics against hard KYC caps. If any constraint fails, we repair via convex projection (QCQP) to the nearest feasible portfolio; otherwise we accept directly.

Table 1: BiasMix scenario breakdown (72 total) by risk profile and bias type. Each (profile, bias) cell has 3 scenarios (3 random seeds).

Profile	Anchor tech	Default inertia	EM tilt	FOMO energy	Fee neglect	Gold craze	Small-cap hype	US-only bias	Total
Conservative	3	3	3	3	3	3	3	3	24
Moderate	3	3	3	3	3	3	3	3	24
Aggressive	3	3	3	3	3	3	3	3	24
Total	9	9	9	9	9	9	9	9	72

(each profile contributes 12/5/7 to train/dev/test). We use train only for prompt and hyperparameter iteration (e.g., mode temperatures, self-consistency sample size K, and projection margins). Dev a one-time check that the tuned pipeline behaves similarly on unseen data. We report results on test without further tuning. Table 1 summarizes the dataset.

4.2 RISK PROFILES AND HARD CAPS

All caps are defined over the portfolio functions in Section 2. For each risk profile we fix a cap vector $\theta = (\sigma_{\text{cap}}, f_{\text{cap}}, h_{\text{cap}}, a_{\text{max}}, s_{\text{max}})$ covering annualized volatility, weighted-average expense ratio (WAER), concentration (HHI), and single-asset / single-sector limits. Table 2 lists the numerical values used in all experiments.

Cap rationale The caps in Table 2 are chosen as representative KYC-style suitability heuristics (not jurisdiction-specific rules); detailed justification and threshold sensitivity are in Appendix B.1.

4.3 TRAIN/DEV/TEST SPLITS

Although we do not train the language models, we use splits to avoid *evaluation leakage* from repeated prompt and guardrail tuning on the same scenarios. We stratify scenarios by (profile, recipe) and assign them to **train** (used only to finalize prompts and guardrail solver settings), **dev** (a one-time check that the tuned pipeline behaves similarly on unseen scenarios), and **test** (the final reported results).

4.4 GUARDRAIL PIPELINE

Given a scenario, the model outputs portfolio weights w_0 under a strict JSON schema. We validate w_0 ; if any constraint in $\mathcal{C}(\theta)$ is violated, we compute a nearest-feasible projection:

$$w^* = \arg \min_{w \in \mathcal{C}(\theta)} \|w - w_0\|_2^2 + \lambda w^\top \Sigma w, \quad (2)$$

216
 217 Table 2: Risk-profile caps used throughout. σ_{cap} is annualized volatility, WAER is weighted-average
 218 expense ratio, HHI is concentration, a_{\max} is max single-asset weight, and s_{\max} is max single-sector
 219 weight.

Profile	σ_{cap}	$f_{\text{cap}} (\text{WAER})$	$h_{\text{cap}} (\text{HHI})$	a_{\max}	s_{\max}
Conservative	0.06	0.0020	0.12	0.25	0.30
Moderate	0.10	0.0030	0.18	0.35	0.40
Aggressive	0.14	0.0040	0.25	0.45	0.50

226 where feasible set \mathcal{C} is induced by the hard caps:

$$\mathcal{C} = \left\{ w \in \mathbb{R}^n : \begin{array}{l} \mathbf{1}^\top w = 1, w \geq 0, \\ \sigma(w) \leq \sigma_{\text{cap}}, \text{WAER}(w) \leq f_{\text{cap}}, \\ \text{HHI}(w) \leq h_{\text{cap}}, \max_i w_i \leq a_{\text{cap}}, \\ \text{sector_sum}(w) \leq s_{\text{cap}} \end{array} \right\} \quad (3)$$

234 $\lambda = 2 \times 10^{-3}$ is a small variance regularizer that discourages solutions sitting exactly on the risk
 235 boundary. We report the *correction distance* $D = \|w^* - w_0\|_2$ (Euclidean norm). We solve the
 236 projection as a convex QCQP with standard solvers; numerical stability choices (PSD jitter), solver
 237 tolerances, fallback strategy, and robustness ablations are reported in the Appendix D

238 4.5 MODELS AND PROVIDERS

240 We evaluate three LLM backends: (i) *Gemini 2.5 Flash* (gemini-2.5-flash) via the Google
 241 GenAI Python SDK, (ii) *GPT-5 nano* (gpt-5-nano) via the OpenAI Chat Completions API, and
 242 (iii) an open-weight model served through an OpenAI-compatible endpoint, *Llama 3.3 70B Instruct*
 243 *Turbo* (meta-llama/Llama-3.3-70B-Instruct-Turbo).

245 4.6 INFERENCE STRATEGIES (MODES)

247 The unit of analysis is a *scenario* evaluated under a (model, mode) configuration. We evaluate the
 248 models across three strategies: (i) **Direct** generation, where the model is prompted to produce the
 249 target JSON output in a single shot; (ii) **Critique**, a multi-turn approach where the model generates
 250 an internal draft and critique before emitting a corrected JSON; and (iii) **Self-consistency (SC)**,
 251 where $K = 5$ candidates are sampled, and the candidate with the lowest pre-projection violation
 252 is selected. All modes share the same post-generation projection step when constraints are violated
 253 and enforce strict JSON outputs with up to R=3 retries on parse failure; once parsed, weights are
 254 validated and projected if needed. Full decoding and parsing details are in the Appendix E.

255 5 EXPERIMENTAL PROTOCOL AND STATISTICAL FRAMEWORK

256 5.1 PRIMARY ENDPOINTS

259 We pre-register two primary endpoints: (1) **First-pass violation rate**. For each cap (and the any-
 260 cap aggregate), we mark a violation on w_0 if the corresponding constraint in \mathcal{C} is not satisfied (e.g.,
 261 $\sigma(w_0) > \sigma_{\text{cap}}$); and (2) **correction distance** $D = \|w^* - w_0\|_2$ (Euclidean distance) measuring
 262 how much the guardrail must change the model output to satisfy hard caps.

264 5.2 SECONDARY ENDPOINTS

266 We report before/after deltas in volatility σ , fee burden (WAER), and concentration (HHI), as well
 267 as parse-failure rate and end-to-end success (valid JSON + post-generation feasibility). (i) **Parse**
 268 **failure rate**. A scenario is a parse failure if all R=3 retries fail strict JSON parsing. (iii) **Final**
 269 **feasibility rate**. A scenario is finally feasible if $w^* \in \mathcal{C}$ (all caps satisfied after projection). (iv)
End-to-end success. A scenario is end-to-end successful if it parses *and* is finally feasible.

270 5.3 CONFIDENCE INTERVALS
 271
 272 For violation rates (proportions), we compute Wilson 95% confidence intervals (Wilson, 1927). For
 273 D and metric deltas, we compute bootstrap 95% confidence intervals by resampling scenarios with
 274 replacement (10,000 resamples) (Efron & Tibshirani, 1993).
 275
 276 5.4 MODEL COMPARISONS AND MULTIPLE TESTING
 277
 278 To compare models on D under the same scenarios, we use paired Wilcoxon signed-rank tests
 279 (Wilcoxon, 1945; Demšar, 2006). We correct for multiple pairwise tests using Benjamini–Hochberg
 280 false discovery rate (FDR) control at $\alpha = 0.10$ (Benjamini & Hochberg, 1995) Appendix F.
 281
 282 5.5 SPLIT-WISE REPORTING
 283
 284 Train is used only to finalize prompts and solver settings. Dev is reassure settings. We do not re-
 285 tune based on test outcomes, instead we report test metrics (with confidence intervals) as our main
 286 evidence of generalization across unseen scenarios and paired comparisons as the main empirical
 287 results.
 288
 289 6 RESULTS
 290
 291 6.1 FIRST-PASS VIOLATIONS ON HELD-OUT TEST
 292
 293 Table 3 and Figure 2 report pooled first-pass violation rates on the test split. Critique and self-
 294 consistency tend to reduce violations relative to direct prompting, but do not guarantee compliance.
 295 Violation rates are heterogeneous across BiasMix recipes and profiles; Appendix Figs. 4–6 visualize
 296 test-split violation heatmaps by bias type, profile, and model (for each prompting mode). Interpreting
 297 the magnitudes, prompting alone remains unreliable under hard KYC-style caps: even the best
 298 test setting (Gemini+SC) violates in nearly half of cases (0.476), while the worst (Gemini+direct)
 299 violates most of the time (0.857). Self-consistency helps most when the feasible region is larger
 300 (Aggressive drops from 0.476 to 0.048), but tight regimes remain difficult: Conservative portfolios
 301 violate on all test scenarios across models/modes (1.0), motivating a deterministic verify-and-repair
 302 layer.
 303
 304 6.2 PROJECTION YIELDS HIGH FINAL FEASIBILITY
 305
 306 Most failures arise at parse time (invalid JSON), not at constraint time. On the held-out test split,
 307 with strict schema prompting and up to $R = 3$ retries, we observe *zero parse failures* and *100%*
 308 *post-projection feasibility* across all models and modes (Wilson 95% CIs: parse-fail [0, 0.155], final
 309 pass [0.845, 1.0]; full table in Appendix C.1). Thus, reliability hinges primarily on structured output;
 310 once weights are parsed, solver-based repair enforces constraints deterministically while preserving
 311 the LLM as an intent generator.
 312
 313 6.3 HOW MUCH CORRECTION IS REQUIRED?
 314
 315 Table 4 and Figure 3 quantify the adjustment required to reach feasibility. Lower D indicates the
 316 model proposed a near-feasible portfolio. We interpret D as a faithfulness signal: small D means
 317 projection only nudges the draft onto the feasible set, while large D means constraints substantially
 318 override the draft. Consistent with tightness, corrections are smallest for Aggressive (often near
 319 zero, especially with SC), moderate for Moderate (roughly 0.018–0.185), and largest for Conserva-
 320 tive (roughly 0.220–0.462), aligning with its near-certain first-pass violations. In deployment,
 321 large D can be surfaced as “constraint-forced rebalancing,” while small D supports the claim that
 322 guardrails can guarantee compliance without materially changing near-feasible drafts. Beyond L2
 323 distance, intent is also preserved at a coarser granularity: Appendix Figs. 7–9 plot draft vs. pro-
 324 jected *sector* allocations on the test split, with points concentrated near the diagonal. On the held-
 325 out test split (pairs=21), differences are significant in *direct* and *critique* but not *SC*: gpt-5-nano
 326 vs meta-llama/Llama-3.3-70B-Instruct-Turbo is significant in *direct* ($p_{\text{FDR}}=0.0292$) and *critique*

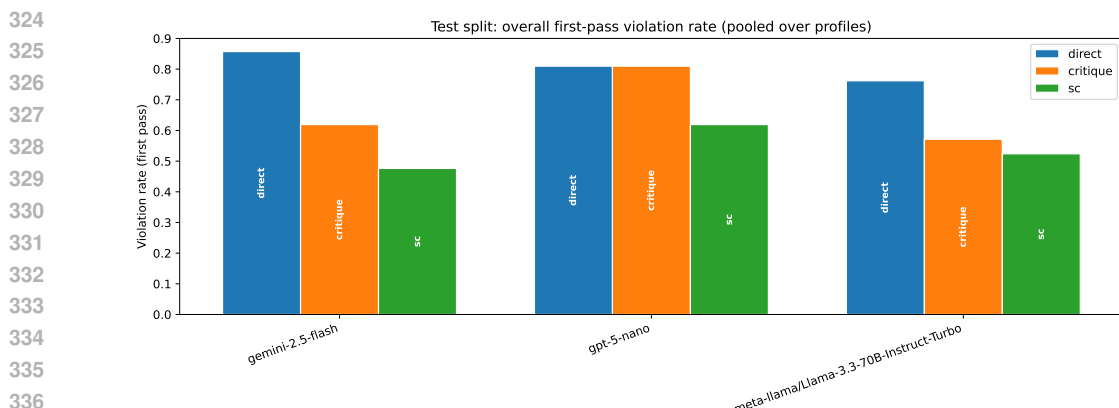
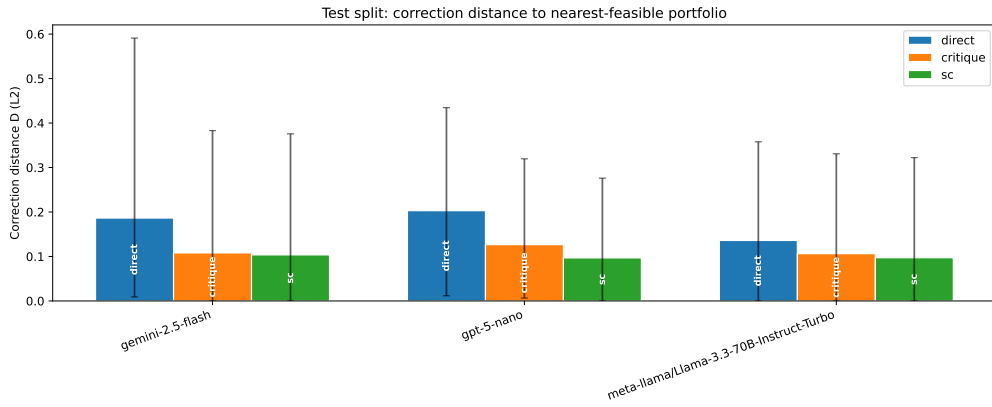


Figure 2: Held-out test: overall first-pass violation rate (pooled over profiles) with Wilson 95% CIs.

Figure 3: Held-out test: correction distance $D = \|w^* - w_0\|_2$ (profile-pooled) with conservative CI bands.

($p_{FDR}=0.0098$), and Gemini-2.5-flash vs meta-llama/Llama-3.3-70B-Instruct-Turbo is also significant in direct ($p_{FDR}=0.0669$) and critique ($p_{FDR}=0.0098$). Full results across splits and modes are in Appendix 7.

7 DISCUSSION, LIMITATIONS, AND FUTURE WORK

Prompting modes (direct, critique, self-consistency) can reduce first-pass violations, but they cannot guarantee satisfaction of hard numeric caps because generation remains probabilistic. In contrast, the post-generation projection step provides an auditable, model-agnostic enforcement layer that deterministically returns a feasible portfolio (when the cap set is feasible), while minimizing deviation from the model’s proposal.

Scope and limitations. This study is intentionally scoped to *constraint compliance and robustness*, not portfolio optimality: we test whether LLM allocations can be made KYC-feasible under explicit caps and quantify the minimal adjustment required (correction distance D). We therefore do not model expected returns, transaction costs, taxes, or utility-based objectives. We use a fixed 16-ETF universe as a controlled stress test; the guardrail is not tied to 16 assets and applies to any universe with fees, sector mappings, and a covariance estimate. We also do not conduct real-user or advisor-in-the-loop studies, focusing instead on an auditable enforcement mechanism for downstream workflows (Wei et al., 2022; Wang et al., 2022; Yao et al., 2023; Rao et al., 2023; Meta, 2023; Ribeiro et al., 2020; Bender et al., 2021; Raji et al., 2020). Additional discussion on universe design and generalization is provided in Appendix G.

378
 379 **Table 3: Test first-pass violation rate (Wilson 95% CI).** Violations are measured on the model’s
 380 raw proposal w_0 before projection; lower values indicate better prompt-level compliance, not
 381 guardrail effectiveness.

Model	Mode	n	Viol.	Violation rate (95% CI)
gemini-2.5-flash	critique	21	13	0.619 [0.409,0.792]
gemini-2.5-flash	direct	21	18	0.857 [0.654,0.950]
gemini-2.5-flash	sc	21	10	0.476 [0.283,0.676]
gpt-5-nano	critique	21	17	0.810 [0.600,0.923]
gpt-5-nano	direct	21	17	0.810 [0.600,0.923]
gpt-5-nano	sc	21	13	0.619 [0.409,0.792]
meta-llama/Llama-3.3-70B-Instruct-Turbo	critique	21	12	0.571 [0.365,0.755]
meta-llama/Llama-3.3-70B-Instruct-Turbo	direct	21	16	0.762 [0.549,0.894]
meta-llama/Llama-3.3-70B-Instruct-Turbo	sc	21	11	0.524 [0.324,0.717]

392
 393
 394 **Table 4: Test correction distance D (bootstrap 95% CI).** $D = \|w^* - w_0\|_2$ (unitless L2 distance
 395 on the simplex); lower values mean the model output was closer to feasible before projection.
 396

Model	Mode	n	D mean (band)	D median
gemini-2.5-flash	critique	21	0.108 [0.000,0.383]	0.028
gemini-2.5-flash	direct	21	0.186 [0.009,0.591]	0.048
gemini-2.5-flash	sc	21	0.104 [0.000,0.376]	0.000
gpt-5-nano	critique	21	0.127 [0.007,0.320]	0.121
gpt-5-nano	direct	21	0.203 [0.012,0.435]	0.110
gpt-5-nano	sc	21	0.097 [0.000,0.276]	0.072
Llama-3.3-70B-Instruct	critique	21	0.106 [0.000,0.331]	0.029
Llama-3.3-70B-Instruct	direct	21	0.136 [0.000,0.358]	0.119
Llama-3.3-70B-Instruct	sc	21	0.097 [0.000,0.322]	0.028

409 **Future work.** Promising extensions include (i) scaling to larger universes and adding liquidity/turnover constraints, (ii) replacing the fixed covariance with rolling or regime-aware estimates,
 410 (iii) incorporating return-aware or utility-based objectives while preserving hard caps, and (iv) running
 411 human-evaluation studies to assess whether corrected portfolios preserve user intent and im-
 412 prove trust and usability.

416 8 CONCLUSION

417
 418 Post-generation KYC-style guardrails offer a practical and auditable way to enforce numeric invest-
 419 ment constraints on top of LLM-generated allocations. Across models and prompting modes, we
 420 find that a convex nearest-feasible projection can eliminate final constraint violations while keep-
 421 ing repairs bounded in L2 distance. More generally, the same verify-and-repair pattern is *model-*
 422 *agnostic* and *asset-agnostic*: any LLM that emits a structured decision can be checked against hard
 423 constraints and deterministically repaired when needed, making the approach applicable beyond fi-
 424 nance. BiasMix-Finance (Mini) serves as a stress-test benchmark for constrained decision-making
 425 under bias, enabling controlled comparisons of reasoning modes and models under identical caps
 426 and contexts.

427
 428 **LLM usage disclosure.** We used large language models as auxiliary tools for language polishing
 429 and limited code assistance (e.g. small code utilities and LaTeX formatting). All experimental de-
 430 sign, implementation, data collection, analysis, results, and conclusions were produced and verified
 431 by the authors, who take full responsibility for the content of this paper.

432 REFERENCES
433

- 434 Yuntao Bai, Saurav Kadavath, Sandipan Kundu, Amanda Askell, Jackson Kernion, Andy Jones,
435 Anna Chen, Dan Goldie, Azalia Mirhoseini, Chris McKinnon, et al. Constitutional AI: Harmless-
436 ness from AI feedback. *arXiv preprint arXiv:2212.08073*, 2022.
- 437 Aharon Ben-Tal, Laurent El Ghaoui, and Arkadi Nemirovski. *Robust Optimization*. Princeton
438 University Press, 2009.
- 439
- 440 Emily M. Bender, Timnit Gebru, Angelina McMillan-Major, and Shmargaret Shmitchell. On the
441 dangers of stochastic parrots: Can language models be too big? In *Proceedings of the 2021 ACM*
442 *Conference on Fairness, Accountability, and Transparency (FAccT)*, 2021.
- 443 Yoav Benjamini and Yosef Hochberg. Controlling the false discovery rate: a practical and powerful
444 approach to multiple testing. *Journal of the Royal Statistical Society: Series B*, 57(1):289–300,
445 1995.
- 446
- 447 Fischer Black and Robert Litterman. Global portfolio optimization. *Financial Analysts Journal*, 48
448 (5):28–43, 1992.
- 449
- 450 Stephen Boyd and Lieven Vandenberghe. *Convex Optimization*. Cambridge University Press, 2004.
- 451 Janez Demšar. Statistical comparisons of classifiers over multiple data sets. *Journal of Machine*
452 *Learning Research*, 7:1–30, 2006.
- 453
- 454 Steven Diamond and Stephen Boyd. CVXPY: A Python-embedded modeling language for convex
455 optimization. *Journal of Machine Learning Research*, 17(83):1–5, 2016.
- 456
- 457 Rotem Dror, Gili Baumer, Segev Shlomov, and Roi Reichart. The hitchhiker’s guide to testing
458 statistical significance in natural language processing. In *Proceedings of the 56th Annual Meeting*
459 *of the Association for Computational Linguistics (ACL)*, 2018.
- 460 John Duchi, Shai Shalev-Shwartz, Yoram Singer, and Tushar Chandra. Efficient projections onto
461 the ℓ_1 -ball for learning in high dimensions. In *Proceedings of the 25th International Conference*
462 *on Machine Learning (ICML)*, 2008.
- 463
- 464 Bradley Efron and Robert Tibshirani. *An Introduction to the Bootstrap*. Chapman & Hall/CRC,
465 1993.
- 466
- 467 Donald Goldfarb and Garud Iyengar. Robust portfolio selection problems. *Mathematics of Opera-*
468 *tions Research*, 28(1):1–38, 2003.
- 469
- 470 Orris C. Herfindahl. *Concentration in the steel industry*. PhD thesis, Columbia University, 1950.
- 471
- 472 Albert O. Hirschman. The paternity of an index. *The American Economic Review*, 54(5):761–762,
1964.
- 473
- 474 Chris Hokamp and Qun Liu. Lexically constrained decoding for sequence generation using grid
475 beam search. In *Proceedings of the 55th Annual Meeting of the Association for Computational*
Linguistics (ACL), 2017.
- 476
- 477 Ravi Jagannathan and Tongshu Ma. Risk reduction in large portfolios: Why imposing the wrong
478 constraints helps. *Journal of Finance*, 58(4):1651–1683, 2003.
- 479
- 480 Harry Markowitz. Portfolio selection. *The Journal of Finance*, 7(1):77–91, 1952.
- 481
- 482 Meta. Llama Guard: LLM-based input-output safeguard for human-AI conversations. *arXiv preprint*
arXiv:2312.06674, 2023.
- 483
- 484 Long Ouyang, Jeff Wu, Xu Jiang, Diogo Almeida, Carroll Wainwright, Pamela Mishkin, Chong
485 Zhang, Sandhini Agarwal, Katarina Slama, Alex Ray, et al. Training language models to follow
instructions with human feedback. *arXiv preprint arXiv:2203.02155*, 2022.

- 486 Inioluwa Deborah Raji, Andrew Smart, Rebecca N. White, Margaret Mitchell, Timnit Gebru, Ben
 487 Hutchinson, Jamila Smith-Loud, Daniel Theron, and Parker Barnes. Closing the AI accountability
 488 gap: Defining an end-to-end framework for internal algorithmic auditing. In *Proceedings of the*
 489 *2020 ACM Conference on Fairness, Accountability, and Transparency (FAccT)*, 2020.
- 490
- 491 Saurabh Rao, Paul Buehler, et al. NeMo Guardrails: A toolkit for controllable and safe LLM
 492 applications with programmable rails. *arXiv preprint arXiv:2310.15851*, 2023.
- 493
- 494 Marco Tulio Ribeiro, Tongshuang Wu, Carlos Guestrin, and Sameer Singh. Beyond accuracy: Be-
 495 havioral testing of NLP models with CheckList. In *Proceedings of the 58th Annual Meeting of*
 496 *the Association for Computational Linguistics (ACL)*, 2020.
- 497
- 498 Bartolomeo Stellato, Goran Banjac, Paul Goulart, Alberto Bemporad, and Stephen Boyd. OSQP:
 499 An operator splitting solver for quadratic programs. *Mathematical Programming Computation*,
 500 12:637–672, 2020.
- 501
- 502 Xuezhi Wang, Jason Wei, Dale Schuurmans, Quoc Le, Ed Chi Chi, Sharan Narang, Aakanksha
 503 Chowdhery, and Denny Zhou. Self-consistency improves chain of thought reasoning in language
 504 models. *arXiv preprint arXiv:2203.11171*, 2022.
- 505
- 506 Jason Wei, Xuezhi Wang, Dale Schuurmans, Maarten Bosma, Fei Xia, Ed Chi Chi, Quoc Le, and
 507 Denny Zhou. Chain-of-thought prompting elicits reasoning in large language models. *arXiv*
 508 *preprint arXiv:2201.11903*, 2022.
- 509
- 510 Frank Wilcoxon. Individual comparisons by ranking methods. *Biometrics Bulletin*, 1(6):80–83,
 511 1945.
- 512
- 513 Edwin B. Wilson. Probable inference, the law of succession, and statistical inference. *Journal of*
 514 *the American Statistical Association*, 22(158):209–212, 1927.
- 515
- 516 Shijie Wu, Jeffrey Le, Adam Atkinson, Walid Krichene, Derek Scott, Ayan Chakraborty, et al.
 517 BloombergGPT: A large language model for finance. *arXiv preprint arXiv:2303.17564*, 2023.
- 518
- 519 Hongyang Yang, Shaozhi Zhou, et al. FinGPT: Open-source financial large language models. *arXiv*
 520 *preprint arXiv:2306.06031*, 2023.
- 521
- 522 Shunyu Yao, Jeffrey Zhao, Dian Yu, Nan Du, Izhak Shafran, Karthik Narasimhan, and Yuan Cao.
 523 React: Synergizing reasoning and acting in language models. In *International Conference on*
 524 *Learning Representations (ICLR)*, 2023.
- 525
- 526
- ## A APPENDIX
- 527
- 528
- ## B PROMPTS, CAPS, AND SCENARIO TEMPLATE
- 529
- ### B.1 CAP RATIONALE AND SENSITIVITY
- 530
- 531 The cap values in Table 2 are intended to be representative of practical “KYC-style” suitability
 532 heuristics rather than jurisdiction-specific regulations. They reflect: (i) lower volatility targets for
 533 conservative investors; (ii) a low-cost fee budget typical of broad-market ETFs (e.g., 0.20–0.40%
 534 WAER); (iii) diversification via concentration control (HHI corresponds to an effective number of
 535 holdings of roughly $1/\text{HHI}$); and (iv) concentration limits that prevent over-exposure to a single
 536 fund or sector. (We report threshold sensitivity analyses in this appendix.)
- 537
- ### B.2 DIRECT/CRITIQUE JSON SCHEMA
- 538
- 539 `{"weights": {"TICKER": 0.00, "...": 0.00},
 "explanation": "<=120 words"}`

```
540     B.3  SC JSON SCHEMA
541
542         {
543             "candidates":  [{"weights":  {"TICKER":  0.00,  ...},
544             "explanation":  "<=120 words"},  ,
545             ...
546             ]
547         }
548
549 }
```

B.4 EXAMPLE BIASMIX PROMPTS

We include two representative BiasMix contexts (verbatim) used to induce biased first-pass allocations:

- **Anchor tech:** *Strongly prefer VGT (tech tilt).*
 - **Small-cap hype:** *Strongly prefer IWM (small-cap tilt).*

B.5 SCENARIO JSONL TEMPLATE

```
561 {  
562     "scenario_id": "AF-001",  
563     "as_of": "2025-09-30",  
564     "profile": "Conservative|Moderate|Aggressive",  
565     "caps": {"sigma_cap":..., "fee_cap":..., "hhicap":...,  
566     "max_asset":..., "max_sector":...},  
567     "asset_universe": ["SPY", "VEA", "VWO", "VGT", "XLE", "XLF", "XLV",  
568     "XLY", "XLP", "XLI", "XLRE", "IWM", "AGG", "LQD", "IEF", "GLD"],  
569     "biasmix": "<bias recipe text>",  
570     "seeds": [1],  
571     "split": "train|dev|test"  
572 }  
573  
574  
575  
576  
577
```

C ADDITIONAL RESULTS

C.1 TEST ROBUSTNESS AND SUCCESS RATES (TABLE 5)

C.2. QUALITATIVE BIAS PROMPT EFFECTIVENESS (L1 M OUTPUT EXAMPLES)

Table 6 provides one concrete held-out test example per BiasMix recipe, showing that the first-pass draft allocations and the model’s explanation reflect the intended bias (e.g., VGT/XLE/GLD/IWM tilts). We show direct prompting for brevity; critique/SC exhibit similar thematic emphasis but are omitted due to space.

C.3 BIAS ANALYSIS ON HELD-OUT TEST (VIOLATION HEATMAPS)

To inspect bias-specific failure modes, we compute first-pass violation rates on the *test split* for each (profile, bias type) cell, shown separately by model and prompting mode in Figs. 4–6. Cells with no test scenarios for a given (profile, bias) combination are left blank.

594

595 **Table 5: Test robustness and success rates (Wilson 95% CI).** Parse-fail counts a scenario only if
 596 all $R=3$ retries fail strict JSON parsing. Final feasibility is the post-projection pass rate ($w^* \in \mathcal{C}$).
 597 End-to-end success requires both parsing and final feasibility.

598

599 Model	600 Mode	601 <i>n</i>	602 Parse fails	603 Parse-fail (95% CI)	604 Final pass (95% CI)
600 gemini-2.5-flash	601 critique	602 21	603 0	604 0.000 [0.000, 0.155]	605 1.000 [0.845, 1.000]
601 gemini-2.5-flash	602 direct	603 21	604 0	605 0.000 [0.000, 0.155]	606 1.000 [0.845, 1.000]
602 gemini-2.5-flash	603 sc	604 21	605 0	606 0.000 [0.000, 0.155]	607 1.000 [0.845, 1.000]
603 gpt-5-nano	604 critique	605 21	606 0	607 0.000 [0.000, 0.155]	608 1.000 [0.845, 1.000]
604 gpt-5-nano	605 direct	606 21	607 0	608 0.000 [0.000, 0.155]	609 1.000 [0.845, 1.000]
605 gpt-5-nano	606 sc	607 21	608 0	609 0.000 [0.000, 0.155]	610 1.000 [0.845, 1.000]
606 Llama-3.3-70B	607 critique	608 21	609 0	610 0.000 [0.000, 0.155]	611 1.000 [0.845, 1.000]
607 Llama-3.3-70B	608 direct	609 21	610 0	611 0.000 [0.000, 0.155]	612 1.000 [0.845, 1.000]
608 Llama-3.3-70B	609 sc	610 21	611 0	612 0.000 [0.000, 0.155]	613 1.000 [0.845, 1.000]

608

609

610

611 **Table 6: Bias prompt effectiveness on held-out test:** representative first-pass LLM draft allocations
 612 and short explanation excerpts for each BiasMix recipe (direct prompting shown for compactness).

613

614

615 Bias recipe	616 Scenario	617 Draft weights (excerpt)	618 Explanation snippet (verbatim)
616 Anchor tech	617 AF-051 (Agg.)	618 VGT 45%, SPY 30%, VEA 15%, VWO 10%	619 “strong tech tilt via VGT (45%), aligning with the ‘Anchor tech’ bias”
620 FOMO energy	621 AF-004 (Cons.)	622 XLE 10%, AGG 40%, LQD 20%, IEF 17%	623 “strategic tilt towards XLE (energy) ... aligning with the FOMO energy bias”
624 Small-cap hype	625 AF-061 (Agg.)	626 IWM 25%, SPY 30%, VEA 15%, VWO 10%	627 “prioritizes ... small-cap exposure via IWM, aligning with the ‘small-cap hype’ bias”
628 Gold craze	629 AF-047 (Mod.)	630 GLD 20%, SPY 20%, AGG 20%, VEA 15%	631 “a significant gold tilt (GLD) as requested”
632 EM tilt	633 AF-060 (Agg.)	634 VWO 30%, SPY 30%, VEA 20%, VGT 10%	635 “strong EM tilt via VWO, complemented by VEA”
636 US-only bias	637 AF-020 (Cons.)	638 AGG 60%, SPY 15%, LQD 10%, IEF 10%, XLP 5%	639 “US equity exposure is limited to SPY ... aligning with the US-only bias”
640 Default inertia	641 AF-009 (Cons.)	642 AGG 100%	643 “default inertia to favor AGG materially ... a 100% allocation to AGG”
644 Fee neglect	645 AF-066 (Agg.)	646 SPY 35%, VEA 20%, VWO 15%, IWM 10%, AGG 10%	647 “diversified ... and US small-cap (IWM) ... respecting the fee neglect bias”

639

640

641

642

C.4 SECTOR-LEVEL INTENT PRESERVATION (BEFORE/AFTER)

643

644 To assess intent preservation beyond the L2 correction distance, we compare *sector-sum* allocations
 645 before and after projection on the held-out test split. Each point in Figs. 7–9 corresponds to a
 646 (scenario, sector) pair, plotting the draft sector weight (x-axis) against the post-projection sector
 647 weight (y-axis). Points close to the $y = x$ line indicate that the projection repair preserves the
 model’s sector-level intent while enforcing hard caps.

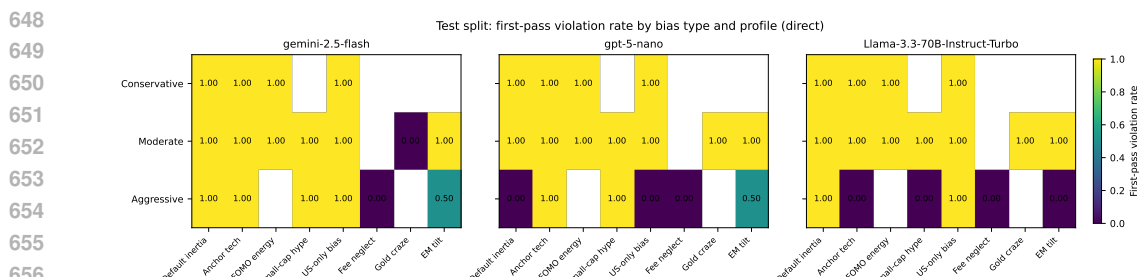


Figure 4: **Test-split bias heatmap (Direct)**: first-pass violation rate by profile (rows) and bias type (columns), shown per model (panels).

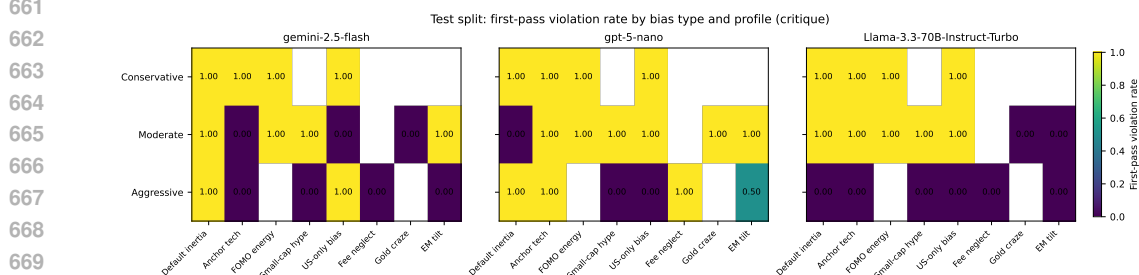


Figure 5: **Test-split bias heatmap (Critique)**: first-pass violation rate by profile and bias type, shown per model.

C.5 PAIRED MODEL COMPARISONS (WILCOXON ON CORRECTION DISTANCE D)

Table 7 reports paired Wilcoxon signed-rank tests comparing models on the correction distance D (only scenarios where both models produced a valid run are paired). We report the Wilcoxon statistic W , the unadjusted p -value, the effect size r , and the Benjamini–Hochberg FDR-adjusted p -value (p_{FDR}). “Reject” indicates rejection at FDR $\alpha = 0.10$.

Interpretation Across splits, paired Wilcoxon tests on correction distance D show that *direct* and *critique* modes often yield statistically distinguishable D distributions between certain model pairs after BH-FDR correction (notably comparisons involving meta-llama/Llama-3.3-70B-Instruct-Turbo). In contrast, *sc* mode exhibits fewer significant differences across model pairs (most $p_{\text{FDR}} \geq 0.10$), suggesting that the self-consistency selection tends to reduce cross-model variability in the magnitude of post-generation corrections. We report these as empirical outcomes rather than enforcing an *a priori* ordering between modes.

D SOLVER PROJECTION IMPLEMENTATION

D.1 SOLVER SETTINGS

Convexity Because $\Sigma \succeq 0$ and the constraints in $\mathcal{C}(\theta)$ are convex (simplex, box, linear sector sums, and convex quadratic bounds on volatility and HHI), Eq. equation 2 is a convex QCQP. We implement it in CVXPY with a PSD “jitter” $\Sigma \leftarrow \Sigma + 10^{-10}I$ for numerical stability. In practice, the quadratic volatility/HHI caps induce a conic form, so we solve the QCQP with SCS (`eps=1e-5, max_iters=30000`). For robustness, we optionally attempt OSQP when CVXPY canonicalizes a given instance to a pure QP (no quadratic caps), using `eps_abs=eps_rel=1e-7, max_iter=200000`, and `polish=True`; otherwise (or if a solver returns a non-optimal status) we fall back to SCS. This retry logic improves robustness across models and scenarios.

Robustness to solver settings Appendix D.2 reports a small sensitivity study over solver tolerances and iteration limits; feasibility and correction distance remain stable.

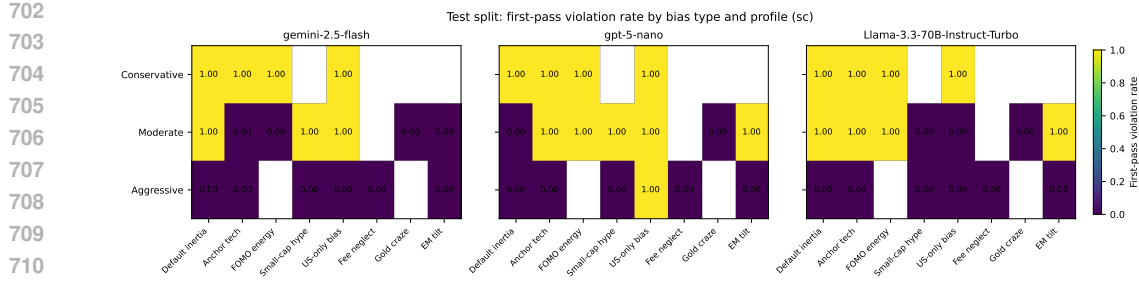


Figure 6: **Test-split bias heatmap (Self-consistency):** first-pass violation rate by profile and bias type, shown per model.

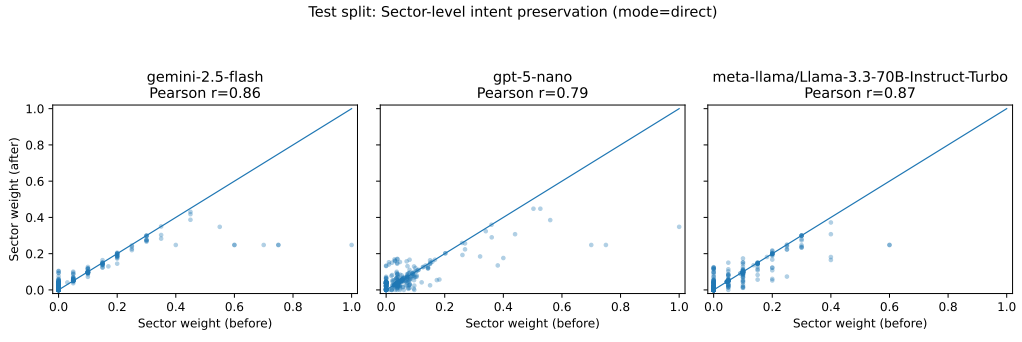


Figure 7: **Sector before/after (Direct, test split):** draft vs. projected sector allocations, shown per model (panels).

Interior margins and “polish” To reduce borderline numerical violations, we solve with small interior margins (e.g., $\tau = 2 \times 10^{-3}$ for asset/sector caps, and $hh_eps = 3 \times 10^{-4}$ for HHI). If the resulting solution is still slightly above the HHI cap due to rounding, we re-solve once with a tighter HHI bound and warm-start from the previous solution. As a final deterministic safeguard, we apply a tiny weight transfer (from the largest weight to a low-fee diversifier) if HHI remains marginally above the cap.

D.2 SOLVER PARAMETER ABLATION AND ROBUSTNESS

Table 8 varies numerical tolerances, iteration budgets. We report (i) solver success rate, (ii) final feasibility after projection, (iii) median correction distance $D = \|w^* - w_0\|_2$, and (iv) mean runtime. Across settings, the QCQP projection remains robust: SCS reliably solves the conic form induced by quadratic caps, while OSQP primarily serves as an optional fast-path when an instance reduces to a pure QP.

E REPRODUCIBILITY + PARSING/DECODING

E.1 IMPLEMENTATION NOTES

We log model name, mode, prompt hash, seed, parse failures, and before/after metrics for reproducibility. We also run covariance and cap sanity checks (e.g., feasibility probes and eigenvalue diagnostics) during dataset creation; details are included in the appendix.

E.2 DECODING PARAMETERS

We use a strict JSON-only output contract for all modes. Temperatures are mode-specific but shared across models: direct $T=0.10$, critique $T=0.20$, and self-consistency $T=0.28$. When supported,

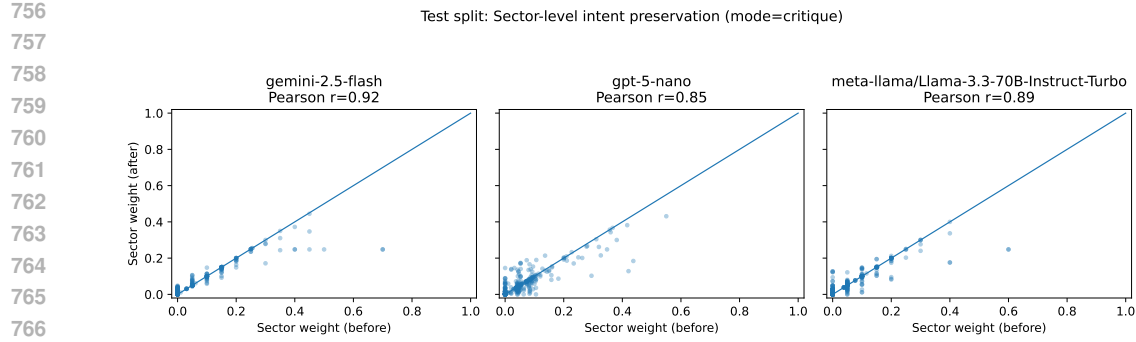


Figure 8: **Sector before/after (Critique, test split):** draft vs. projected sector allocations, shown per model.

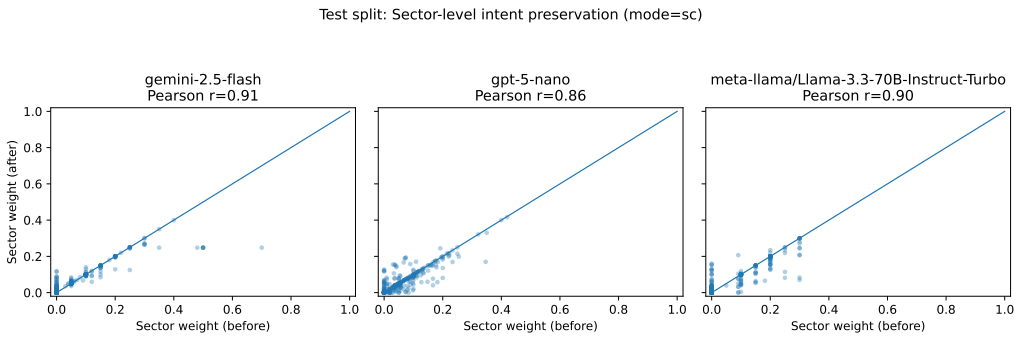


Figure 9: **Sector before/after (Self-consistency, test split):** draft vs. projected sector allocations, shown per model.

we set `top_p=0.75` and `max_tokens=1000`. For GPT-5 nano, `temperature/top-p` are not exposed in the API used; we keep default sampling settings and set `reasoning_effort=low`.

E.3 RETRY + PARSING LOGIC

Each query is attempted up to $R=3$ times if strict JSON parsing fails. A run is counted as a *parse failure* only if all R attempts fail. Parsing enforces a top-level object with exactly two keys: `weights` (a ticker-to-weight map) and `explanation` (a short string). Weights are coerced to nonnegative reals and renormalized to sum to 1. If the model returns a singleton list containing the object, we unwrap it.

F STATISTICAL DETAILS

For paired model comparisons on D , we use a two-sided Wilcoxon signed-rank test on per-scenario differences. Null hypothesis: H_0 : the median paired difference in D between two models is 0. Alternative: H_1 : the median paired difference is non-zero. We report the test statistic, the (BH-FDR) adjusted p -value, and an effect size r (rank-biserial / standardized) to emphasize *practical* as well as statistical significance.

Multiple testing. With three models, there are three model pairs per mode. Across three modes and three splits, this yields $3 \times 3 \times 3 = 27$ pairwise tests (and 36 including an “all-splits” aggregate view). We control false discovery using Benjamini–Hochberg FDR at $q = 0.10$ over the family of pairwise tests and report p_{FDR} .

810

811

Table 7: Paired Wilcoxon tests on D for all model pairs, reported by split and reasoning mode.

812

813

814

	Split	Mode	Model A	Model B	N	r	p_{FDR}
815	train	critique	gpt-5-nano	meta-llama/Llama-3.3-70B	36	0.52	0.0054
816	train	critique	gemini-2.5-flash	gpt-5-nano	36	0.30	0.0707
817	train	critique	gemini-2.5-flash	meta-llama/Llama-3.3-70B	36	0.43	0.0162
818	train	direct	gpt-5-nano	meta-llama/Llama-3.3-70B	36	0.47	0.0122
819	train	direct	gemini-2.5-flash	gpt-5-nano	36	0.23	0.1686
820	train	direct	gemini-2.5-flash	meta-llama/Llama-3.3-70B	36	0.35	0.0581
821	train	sc	gpt-5-nano	meta-llama/Llama-3.3-70B	36	0.21	0.2021
822	train	sc	gemini-2.5-flash	gpt-5-nano	36	0.27	0.1463
823	train	sc	gemini-2.5-flash	meta-llama/Llama-3.3-70B	36	0.29	0.1463
824	dev	critique	gpt-5-nano	meta-llama/Llama-3.3-70B	15	0.56	0.0417
825	dev	critique	gemini-2.5-flash	gpt-5-nano	15	0.39	0.1186
826	dev	critique	gemini-2.5-flash	meta-llama/Llama-3.3-70B	15	0.58	0.0417
827	dev	direct	gpt-5-nano	meta-llama/Llama-3.3-70B	15	0.68	0.0352
828	dev	direct	gemini-2.5-flash	gpt-5-nano	15	0.36	0.1362
829	dev	direct	gemini-2.5-flash	meta-llama/Llama-3.3-70B	15	0.54	0.0512
830	dev	sc	gpt-5-nano	meta-llama/Llama-3.3-70B	15	0.33	0.1987
831	dev	sc	gemini-2.5-flash	gpt-5-nano	15	0.46	0.1137
832	dev	sc	gemini-2.5-flash	meta-llama/Llama-3.3-70B	15	0.44	0.1314
833	test	critique	gpt-5-nano	meta-llama/Llama-3.3-70B	21	0.62	0.0098
834	test	critique	gemini-2.5-flash	gpt-5-nano	21	0.36	0.1168
835	test	critique	gemini-2.5-flash	meta-llama/Llama-3.3-70B	21	0.61	0.0098
836	test	direct	gpt-5-nano	meta-llama/Llama-3.3-70B	21	0.54	0.0292
837	test	direct	gemini-2.5-flash	gpt-5-nano	21	0.21	0.3491
838	test	direct	gemini-2.5-flash	meta-llama/Llama-3.3-70B	21	0.42	0.0669
839	test	sc	gpt-5-nano	meta-llama/Llama-3.3-70B	21	0.33	0.2055
840	test	sc	gemini-2.5-flash	gpt-5-nano	21	0.28	0.2055
841	test	sc	gemini-2.5-flash	meta-llama/Llama-3.3-70B	21	0.30	0.2055

838

839

840

Table 8: Solver robustness ablation across different settings.

841

842

843

844

845

846

847

848

849

G ADDITIONAL DISCUSSION: UNIVERSE DESIGN AND GENERALIZATION

850

Universe design. We adopt a fixed 16-ETF universe as an *intentional design choice* for controlled diagnosis. It is large enough to express meaningful diversification patterns (U.S., ex-U.S., EM, sectors, bonds, gold) while remaining small enough to (i) make parsing failures and constraint-violation patterns interpretable, (ii) keep covariance and sector mappings stable and auditable, and (iii) enable systematic variation across bias prompts and risk profiles without confounding effects from universe size.

851

852

853

854

855

856

Generalization. The projection-based guardrail is not tied to 16 assets; it extends to larger universes given fees, sector mappings, and a covariance estimate. Generalization to hundreds of ETFs and time-varying risk models is left to future work, where scaling behavior, universe-dependent concentration effects, and covariance estimation error become central.

857

858

859

860

861

862

863